

# BATTERY RECYCLING: EFFECT OF CURRENT DENSITY ON MANGANESE RECOVERY THROUGH ELECTROLYTIC PROCESS

E. R. R. Roriz<sup>1</sup>, D. C. R. Espinosa<sup>2</sup> and J. A. S. Tenório<sup>2\*</sup>

<sup>1</sup>Instituto Federal do Espírito Santo, Av. Vitória 1729, CEP: 29040-780, Vitória - ES, Brazil.

<sup>2</sup>Escola Politécnica, University of São Paulo, Department of Chemical Engineering, Av. Prof. Lineu Prestes 580, Bloco 18, Conjunto das Químicas, CEP: 05508-000, São Paulo - SP, Brazil.

E-mail: jtenorio@usp.br

(Submitted: June 19, 2014 ; Revised: December 24, 2014 ; Accepted: February 19, 2015)

**Abstract** - This work aims to verify the possibility of using depleted batteries as a source of manganese dioxide applying the electrolytic process. An electrolyte solution containing the following metal ions was used: Ca (270 mgL<sup>-1</sup>), Ni (3.000 mgL<sup>-1</sup>), Co (630 mgL<sup>-1</sup>), Mn (115.3 mgL<sup>-1</sup>), Ti (400 mgL<sup>-1</sup>) and Pb (20 mgL<sup>-1</sup>). The production of electrolytic manganese dioxide (EMD) was performed through electrolysis at 98 °C (± 2 °C) applying different current densities (ranging from 0.61 A.dm<sup>-2</sup> to 2.51 A.dm<sup>-2</sup>). The materials obtained were analyzed through X-ray fluorescence spectrometry, X-ray diffraction, specific surface area (BET) and scanning electron microscopy (SEM). The best results regarding the current efficiency, purity grade and specific surface area were obtained with a current density ranging between 1.02 A.dm<sup>-2</sup> and 1.39 A.dm<sup>-2</sup>. The allotropic ε-MnO<sub>2</sub> variety was found in all tests.

**Keywords:** Batteries; Recycling; Manganese dioxide.

## INTRODUCTION

Electrolytic manganese dioxide (EMD) is the main active component present in the cathodes of several cell systems. The most common system among those using manganese dioxide is the system of primary alkaline batteries Zn/MnO<sub>2</sub>. This component is also found in the aqueous system of zinc-carbon batteries and in some lithium batteries. Currently, manganese dioxide has been investigated as a precursor in the production of spinel (LiMn<sub>2</sub>O<sub>4</sub>), one of the main components to be used as cathodic material for rechargeable lithium batteries (Strobel *et al.*, 2003; Komaba *et al.*, 2005). Recycling of batteries has been studied in recent years, but the recovery of materials present remains a challenge (Espinosa, *et al.*, 2004; Bernardes *et al.*, 2004; Espinosa and Tenório, 2004; Espinosa and Tenório, 2006).

The use of electrolytic manganese dioxide in the alkaline battery industry exceeded 23.000 t/year in 2.002 (Zhang and Cheng, 2007). The high consumption of this substance is because of the growing demand for batteries in the market worldwide, generated by the mass production and consumption of portable electronic devices such as digital cameras, telephones, computers and high-tech toys, whose power supplies are almost exclusively batteries based on a Zn/MnO<sub>2</sub> system. These cells represent a significant percentage of the total number of batteries available in the market, mainly due to the characteristics of the manganese dioxide cathode performance (Browning and Donne, 2005) and its low cost.

Because of the growing need for products containing manganese, the use of secondary sources of this metal has become increasingly necessary. For this purpose, studies have been done on: the use of

\*To whom correspondence should be addressed

low-grade manganese ores (lower than 40%), of ocean manganese nodules and manganese-containing materials such as steel scrap, spent electrodes, used catalysts, and spent batteries (Zhang and Cheng, 2007).

Considering these studies, this work focuses on the recovery of manganese from spent batteries, which is feasible due to the high content of manganese dioxide (28 to 38 wt.%) present in the composition of cells produced with this material.

The hydrometallurgical process has been widely used for separation of the metals contained in batteries (Sayilgan *et al.*, 2009; Li *et al.*, 2009; Vatistas *et al.*, 2001; Provazi *et al.*, 2011). The solution from the hydrometallurgical treatment process for battery recycling can be a potentially important source of manganese.

The objective of this work focuses on the electrolytic process for recovering the manganese present in the sulfuric leaching liquor of exhausted batteries.

## MATERIALS AND METHODS

The purpose of this study was to obtain electrolytic manganese dioxide from the synthetic solution prepared, taking into consideration results obtained elsewhere (Provazi *et al.*, 2011). Provazi *et al.* (2011) studied the sulfuric acid leaching of a mixture of household batteries from a municipal collection box.

### Electrolytic Solution Preparation

The reagents used in the solution preparation were cobalt sulfate heptahydrate (Merck PA), manganous sulfate monohydrate (Proquimios PA), calcium sulfate dehydrate (Carlo Erba PA), nickel sulfate hexahydrate (Vetec PA), lead sulfate (Aldrich PA), titanium (IV) oxide (Vetec) and sulfuric acid (Vetec).

The solution was prepared by adding the following reagents:  $\text{MnSO}_4 \cdot \text{H}_2\text{O}$ ,  $\text{CoSO}_4 \cdot 7\text{H}_2\text{O}$ ,  $\text{CaSO}_4 \cdot 2\text{H}_2\text{O}$ ,  $\text{NiSO}_4 \cdot 6\text{H}_2\text{O}$ ,  $\text{PbSO}_4$ , concentrated  $\text{H}_2\text{SO}_4$ , solution of titanium and enough Mili-Q water (a water purification system that involves steps of filtration and deionization) to complete a liter of the solution. The amount of each reagent added was calculated to provide the ions and the pH value corresponding to the solution found in a previous study (Provazi *et al.*, 2011).

Table 1 provides the values of concentrations in  $\text{mgL}^{-1}$  of metal ions and the final pH of the electrolytic solution.

**Table 1: Composition of electrolyte solution.**

Reactant	Metallic ion	Ion conc. (mg/L)	pH
$\text{MnSO}_4 \cdot \text{H}_2\text{O}$	$\text{Mn}^{2+}$	115, 300	0.3
$\text{CoSO}_4 \cdot 7\text{H}_2\text{O}$	$\text{Co}^{2+}$	630	
$\text{CaSO}_4 \cdot 2\text{H}_2\text{O}$	$\text{Ca}^{2+}$	270	
$\text{NiSO}_4 \cdot 6\text{H}_2\text{O}$	$\text{Ni}^{2+}$	3000	
$\text{PbSO}_4$	$\text{Pb}^{2+}$	20	
$\text{TiO}_2$	Acid solution $\text{TiO}^{2+}$	400	

### Electrolysis Tests

The cell used during the electrolytic process consisted of a 250 mL beaker, for which a special round plastic lid was created. The lid contains openings to hold: two counter electrodes, a working electrode, a thermometer and a condenser, as shown in Figure 1 and Figure 2. A lead plate 5.0 cm high, 2.0 cm wide and 0.1 cm thick was used as the working electrode (anode) and two graphite plates 2.5 cm high, 1.0 cm wide, and 0.5 cm thick as counter electrode (cathode).

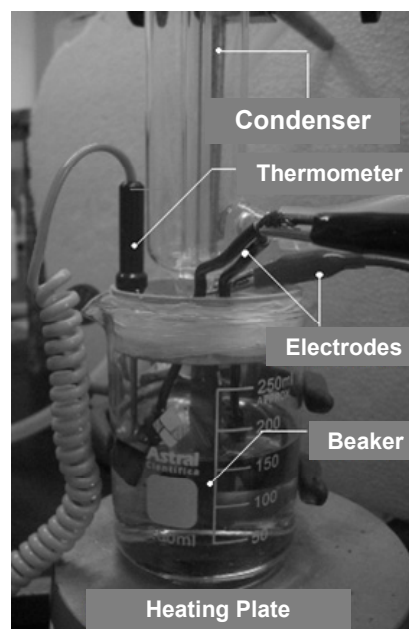


**Figure 1:** Electrochemical cell developed for production of EMD.

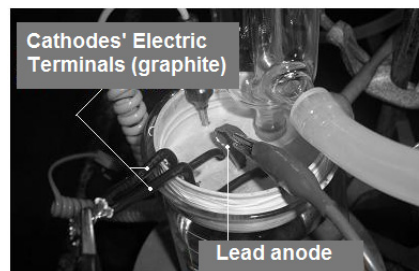


**Figure 2:** In detail, the lid of the electrolytic cell.

Five samples of electrolyte solution with pH 0.30, containing 150 mL each, were anodically electrolyzed during 4 hours, at a temperature of 98 °C ( $\pm 2$  °C). For each sample, a different range of current density was used, varying from 0.61 to 2.51 A.dm<sup>-2</sup>. After each test, the anode was removed from the electrolytic cell and washed with Mili-Q water and dried at 100 °C. EMD deposits were mechanically removed from the anode and were repeatedly washed with Mili-Q water. Afterwards, the EMD was dried at a temperature of 100 °C. Table 2 contains a summary of the tests performed.

**Table 2: Tests and parameters used in the electrolysis tests performed at different current densities.**

Tests	J (A.dm <sup>-2</sup> )	Temp. (°C)	Time (h)
DMEJ 0.61	0.61	98	4
DMEJ 1.02	1.02		
DMEJ 1.39	1.39		
DMEJ 1.93	1.93		
DMEJ 2.51	2.51		

### Characterization

The characterization of the EMD deposits, collected from the anodes was performed to identify the characteristics of the product obtained.

The following techniques were used: X-ray fluorescence spectrometry, X-ray diffraction, determination of specific surface area by the BET method and scanning electron microscopy (SEM).

As samples were composed of oxides, it was necessary to sputter all samples with gold. Consequently, this element appeared in the spectrum when EDS analysis was carried out.

## RESULTS AND DISCUSSION

### Current Efficiency

The anodic current efficiency behavior during the electrolytic process was analyzed varying the current density. Figure 3 shows the anodic current efficiency for tests performed at different current densities.

The current efficiency in the process for obtaining manganese dioxide initially rose with increasing current density, achieving a maximum (94.3%), and then decreased. The maximum efficiency was noted at the current density of 1.02 A.dm<sup>-2</sup>, which is the value usually adopted in the industrial process for obtaining EMD. A sharp decrease of current efficiency (70.5%) with increasing current density (2.51 A.dm<sup>-2</sup>) was noticed. This variation of current

efficiency takes place because, under high current density, the electrolysis of water occurs and the evolution of oxygen can become a competitive reaction in place of the deposition of manganese dioxide, reducing the current efficiency (Ghaemi and Binder, 2002).

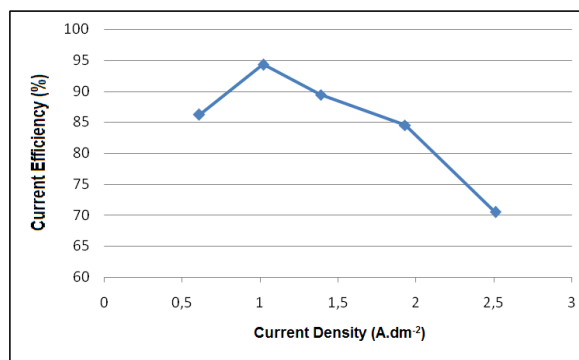


**Figure 3: Effect of current density on the anodic current efficiency in tests for the production of EMD.**

Another aspect that should be considered is the fact that, under high current density, the rate of deposition is higher than the transport of ions to the electrode and the concentration of metal ions near the anode is reduced (Ghaemi and Binder, 2002).

These results are close to those found by Ghaemi and Binder (2002), who verified that efficiencies higher than 90% (from 91 to 99%) can be obtained at a current density of around 1 A.dm<sup>-2</sup>. A current efficiency of 80% was obtained in the range of 1.35 A.dm<sup>-2</sup> to 1.39 A.dm<sup>-2</sup> and at a very high density such as 3.75 A.dm<sup>-2</sup>, the current efficiency decreased to 36%.

### Specific Surface Area

The values of specific surface area obtained through the BET method in the EMD samples produced at different current densities, are shown in Figure 4.

The results showed that the specific surface area of EMD grows with increasing current density from 0.61 A.dm<sup>-2</sup> (131.54 m<sup>2</sup>.g<sup>-1</sup>) to 1.02 A.dm<sup>-2</sup> (150.85 m<sup>2</sup>.g<sup>-1</sup>) and the specific surface area of EMD remained almost constant from this point until the current density of 1.93 A.dm<sup>-2</sup> (150.85 m<sup>2</sup>.g<sup>-1</sup>, 154.44 m<sup>2</sup>.g<sup>-1</sup>, 145.95 m<sup>2</sup>.g<sup>-1</sup>). At the current density of 2.51 A.dm<sup>-2</sup>, against all expectations, there was a dramatic decrease in specific surface area (128.7 m<sup>2</sup>.g<sup>-1</sup>). This result may have been due to ineffective control of the variables of the process during the execution of the experiment for this sample.

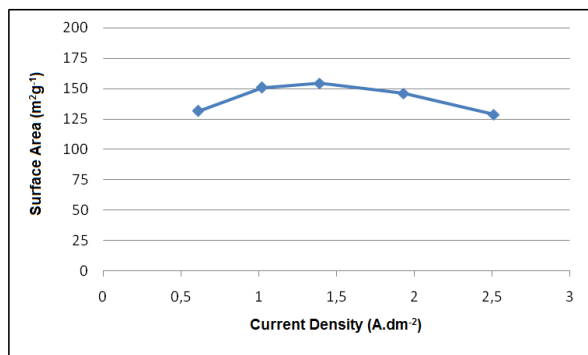


**Figure 4:** Effect of current density on the surface area of electrolytic manganese dioxide.

Davis *et al.* (2001) state that the EMD is a dense solid with significant internal porosity, which leads to a large BET surface area (20 – 100 m<sup>2</sup>.g<sup>-1</sup>).

The increase in the specific surface area with the current density is presumably due to a high nucleation rate with high current density, which results in many small primary particles (Tamura *et al.*, 1997).

### Chemical Analysis

The chemical composition of EMD samples produced at different current densities is shown in Table 3.

The range used for the variation of current density (0.61 A.dm<sup>-2</sup> to 2.51 A.dm<sup>-2</sup>) does not significantly affect the content of MnO<sub>2</sub> present in the final products, which showed levels above 90%.

**Table 3: Results of chemical analysis by X-ray fluorescence spectrometry of the EMD samples obtained at different current densities (in mass percentage).**

Composition	J=0.61 A.dm <sup>-2</sup>	J=1.02 A.dm <sup>-2</sup>	J=1.39 A.dm <sup>-2</sup>	J=1.93 A.dm <sup>-2</sup>	J=2.51 A.dm <sup>-2</sup>
F	1.89	1.73	1.73	nd	1.38
Na	nd	nd	nd	nd	nd
Al	nd	0.01	0.01	0.01	0.01
Si	0.01	0.03	0.07	0.02	0.03
P	<<	<<	<<	<<	0.01
S	1.33	0.64	0.78	0.94	0.57
K	0.14	0.15	0.18	0.22	0.20
Ca	0.01	0.01	nd	0.01	nd
Ti	0.67	0.63	0.52	0.52	0.84
MnO <sub>2</sub>	94.98	95.44	95.83	97.35	96.00
Fe	0.13	0.16	0.12	0.13	0.14
Co	0.20	0.15	0.08	0.14	0.11
Ni	0.14	0.09	0.12	0.10	0.09
Zn	nd	nd	nd	0.02	nd
Pb	0.50	0.96	0.56	0.54	0.62

Comparing these results with the specifications of commercial electrolytic manganese dioxide, in regard

to the concentration of MnO<sub>2</sub>, the results obtained were in accordance with the specifications required for use in battery production where 91% MnO<sub>2</sub> (dry basis) is the minimum concentration of MnO<sub>2</sub> allowed.

Analyzing the impurities present in the results, there was contamination in the materials obtained by the electrolytic process. Such contamination is due to the impurities in the chemicals used for the solution preparation.

### X-Ray Diffraction

Figure 5 shows a typical X-ray diffractogram obtained in the tests performed at current densities of 0.61 A.dm<sup>-2</sup>, 1.02 A.dm<sup>-2</sup>, 1.93 A.dm<sup>-2</sup>, 1.39 A.dm<sup>-2</sup>, and 2.51 A.dm<sup>-2</sup> after a 4-hour period, at a temperature of 98 °C. The X-ray diffraction analyses of all samples presented consistent results for the crystallographic file JCPDS 30-0820, referring to the ε-MnO<sub>2</sub> allotropic form. The ε-MnO<sub>2</sub> phase is the desirable allotropic form of EMD usually used in batteries.

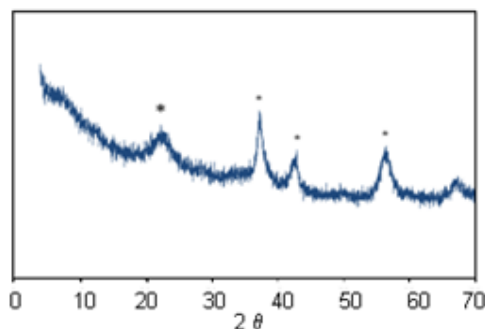


**Figure 5:** X-ray diffraction pattern of EMD obtained at 98 °C after 4h of test (\*ε - MnO<sub>2</sub>).

### Scanning Electron Microscopy

Figure 6 shows features of the surfaces of particles deposited on the lead electrode at different anodic current densities after a 4 hour period.

The surfaces of EMD samples were covered with fine cracks that appeared when the deposits were cooled after the removal from the hot solution. A greater number of cracks in the deposits were especially observed (Figure 6e) at higher current density (2.51A.dm<sup>-2</sup>). The increase in the current density caused an increase in the thickness of the deposit. The observed cracks on the surface of the deposit should be a consequence of the handling of a thicker material.

The increase in current density leads to the formation of slightly dendritic deposits, as shown in

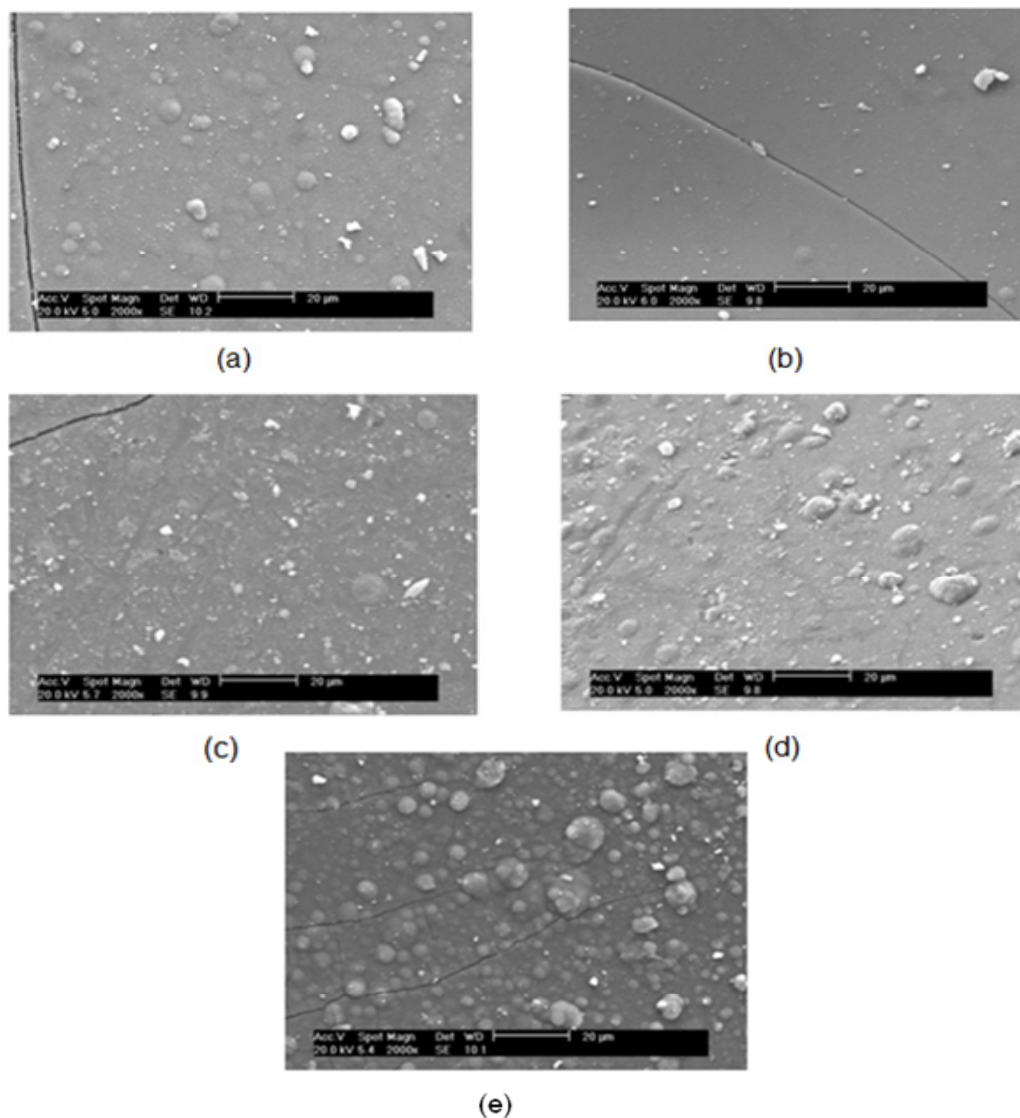
Figure 6 (d and e). The deposits obtained at lower current density presented a smoother surface aspect, as shown in Figure 6a and 6b; however, the deposit obtained at a current density of  $1.02 \text{ A.dm}^{-2}$  showed a structure with fairly smooth appearance (Figure 6b).

Figure 7 shows a typical EDS spectra of the surface of EMD produced at different anodic current densities.

The EDS spectra were similar. Manganese was indicated as the predominant element in the composition of the electroplated material obtained. This fact is compatible with the chemical analysis carried

out earlier.

The spectra also present peaks of lead and titanium as contaminants in the EMD. This result indicates that Ti oxide is carried to the deposit during the electrolysis. In all samples, the presence of lead was greater than that of titanium. Lead contamination in the EMD could occur when the deposit is removed. This can be seen in Figure 8, which shows the face of the deposited material that is in contact with the electrode. In this image, the white area (A) is predominantly composed of lead, and a dark area can be seen (B), which is predominantly composed of manganese.



**Figure 6:** Back-scattered electron image. Morphology of  $\text{MnO}_2$  electrodeposited on the lead electrode at different current densities: a)  $0.61 \text{ A.dm}^{-2}$  b)  $1.02 \text{ A.dm}^{-2}$  c)  $1.39 \text{ A.dm}^{-2}$  d)  $1.93 \text{ A.dm}^{-2}$  e)  $2.51 \text{ A.dm}^{-2}$ .

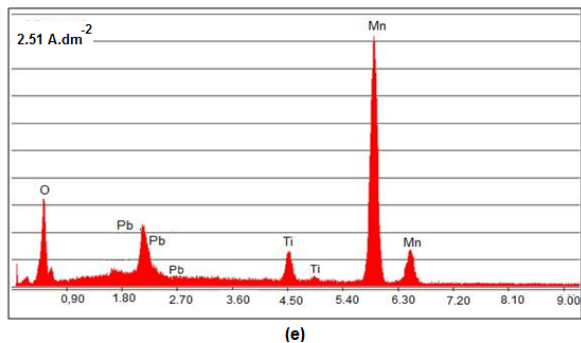


**Figure 7:** EDS spectra of the material deposited on the lead electrode at a current density of  $2.51 \text{ A.dm}^{-2}$ .

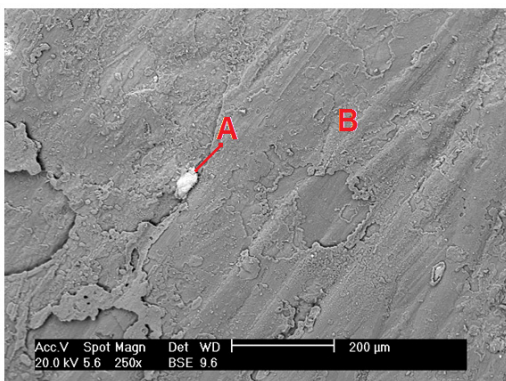


**Figure 8:** Back-scattered electron image. Morphology of DME produced using  $2.51 \text{ A.dm}^{-2}$ .

The industrial production of EMD involves the sulfuric acid leaching of manganese dioxide ores followed by the electrowinning of the solution, producing 92% purity manganese dioxide in the cathodes. The process is basically the same studied in this paper to produce EMD.

The main difference is the material of the leaching process. In the industrial process a primary source is used and, in this approach, a secondary source material produces the same product. Consequently, the main purpose is to reduce the use of primary raw materials. As the process is essentially the same, *e.g.*, the same reactants and the same processing conditions in the electrowinning step, the overall cost of EMD production using batteries instead of manganese ores should be the same.

## CONCLUSIONS

1. The best values of current efficiency (94.3% and 89.4%) and of specific surface area ( $150.9 \text{ m}^2.\text{g}^{-1}$  and  $131.5 \text{ m}^2.\text{g}^{-1}$ ) were obtained by applying current densities from  $1.02 \text{ A.dm}^{-2}$  to  $1.39 \text{ A.dm}^{-2}$ .

2. The EMD samples, obtained with current density ranging from  $0.61 \text{ A.dm}^{-2}$  to  $2.51 \text{ A.dm}^{-2}$ , presented more than 90 wt.% of  $\epsilon$ - $\text{MnO}_2$ .

3. The best results regarding the concentration of  $\text{MnO}_2$  (97.4%) were obtained in the samples produced with a current density of  $1.93 \text{ A.dm}^{-2}$ .

4. Variation of the current density from  $0.61 \text{ A.dm}^{-2}$  to  $2.51 \text{ A.dm}^{-2}$  did not affect the structure of the EMD obtained. In all samples, there was a predominance of  $\epsilon$ - $\text{MnO}_2$ .

## REFERENCES

- Bernardes, A. M., Espinosa, D. C. R., Tenório, J. A. S., Recycling of batteries: A review of current processes and technologies. *Journal of Power Sources*, 130(1-2), 291-298 (2004).
- Browning, J. G., Donne, W. S., Electrochemical kinetic behaviour of the aqueous manganese dioxide electrode. *Journal of Applied Electrochemistry*, 35, 437-443 (2005).
- Davis, S. M., Bowden, W. L., Richards, T. C., Defining high power EMD through porosimetry. *Journal of Power Sources*, 139, 342-350 (2005).
- Espinosa, D. C. R., Tenório, J. A. S., Recycling of nickel-cadmium batteries using coal as reducing. *Journal of Power Sources*, 157, 600-604 (2006).
- Espinosa, D. C. R., Bernardes, A. M., Tenório, J. A. S., An overview on the current processes for the recycling of batteries. *Journal of Power Sources*, 135(1-2), 311-319 (2004).
- Espinosa, D. C. R., Tenório, J. A. S., Fundamental aspects of the recycling of nickel-cadmium batteries through vacuum distillation. *Journal of Power Sources*, 135(1-2), 320-326 (2004).
- Ghaem, M., Binder, L., Effects of direct and pulse current on electrodeposition of manganese dioxide. *Journal of Power Sources*, 111, 248-254 (2002).
- Komaba, S., Sasaki, T., Kumagai, N., Preparation and electrochemical performance of composite oxide of alpha manganese dioxide and Li-Mn-O spinel. *Electrochimica Acta*, 50, 2297-2305 (2005).
- Li, J., Li, X., Hu, Q., Wang, Z., Zheng, J., Wu, L., Zhang, L., Study of extraction and purification of Ni, Co and Mn from spent battery material. *Hydrometallurgy*, 99, 7-12 (2009).
- Provazi, K., Campos, B. A., Espinosa, D. C. R., Tenório, J. A. S., Metal separation from mixed types of batteries using selective precipitation and liquid liquid extraction techniques. *Waste Management*, 31, 59-64 (2011).
- Sayilgan, E., Kukrer, T., Ferella, F., Veglio, F., Kitis, M., Reductive leaching of manganese and zinc

- from spent alkaline and zinc-carbon batteries in acidic media. *Hydrometallurgy*, 97, 73-79 (2009).
- Strobel, P., Ibarra-Palos, A., Anne, M., Poinsignon, C., Crisci, A., Cation ordering in  $\text{Li}_2\text{Mn}_3\text{MO}_8$  spinels: Structural and vibration spectroscopy studies. *Solid State Sciences*, 5, 1009-1018 (2003).
- Vatistas, N., Bartolozzi, M., Arras, S., The dismantling of the spent alkaline zinc manganese dioxide batteries and the recovery of the zinc from the anodic material. *Journal of Power Sources*, 101, 182-187 (2001).
- Tamura, H., Ishizeki, K., Nagayama, M., Furuichi, R., Incorporation of impurity metal ions in electrolytic manganese dioxide. *Journal of Electrochemistry Society*, 8, 141-147 (1994).
- Zhang, W., Cheng, Y. C., Manganese metallurgy review. Part I: Leaching of ores/secondary materials and recovery of electrolytic/chemical manganese dioxide. *Hydrometallurgy*, 89, 137-159 (2007).